stimulation of poly(ADP-ribose) by UV irradiation or MNNG treatment results in a rapid depletion of cellular NAD^+ levels which may render the cells unable to maintain their redox state and energy metabolism. Thus, the rapid depletion of NAD^+ may lead to a metabolic cell death before the DNA repair processes can be completed. The effect of nicotinamide and the NAD^+ analogues could be to slow down the reduction in NAD^+ levels so that the cells maintain sufficient pyridine nucleotide coenzymes to continue energy metabolism and repair DNA under more controlled conditions.

References

Althaus, F. R., Lawrence, S. D., Sattler, G. L., & Pitot, H. C. (1980) *Biochem. Biophys. Res. Commun. 95*, 1063–100.

Benjamin, R. C., & Gill, D. M. (1980) *J. Biol. Chem. 225*, 10493–10501.

Berger, N. A., & Sikorski, G. W. (1980) *Biochem. Biophys. Res. Commun. 95*, 67–72.

Berger, N. A., Sikorski, G. W., & Petzold, S. J., & Kurohara, K. K. (1979) *J. Clin. Invest. 63*, 1164–1171.

Butt, T. F., Brothers, J. F., Giri, C. P., & Smulson, M. E. (1978) *Nucleic Acids Res. 5*, 2775–2788.

Collins, A. R. S., Schor, S. L., & Johnson, R. T. (1977) *Mutat. Res. 42*, 413–432.

Cornelis, J. J. (1978) *Biochim. Biophys. Acta 521*, 134–143.

Durkacz, B. W., Omidiji, O., Gray, D. A., & Shall, S. (1980) *Nature (London) 283*, 593–596.

Durkacz, B. W., Irwin, J., & Shall, S. (1981) *Biochem. Biophys. Res. Commun. 101*, 1433–1441.

Francis, A. A., Blevins, R. D., Carrier, W. L., Smith, D. P., & Regan, J. D. (1979) *Biochim. Biophys. Acta 563*, 385–392.

Goodwin, P. M., Lewis, P. J., Davis, M. I., Skidmore, C. J., & Shall, S. (1978) *Biochim. Biophys. Acta 543*, 576–582.

Hayaishi, O., & Ueda, K. (1977) *Annu. Rev. Biochem. 46*, 95–116.

Hilz, H., & Stone, P. (1976) *Rev. Physiol., Biochem. Pharmacol. 76*, 1–58.

Jacobson, E. L., Juarez, D., & Sims, J. L. (1980) *Fed. Proc., Fed Am. Soc. Exp. Biol. 39 (No. 6)*, 1739A.

Jacobson, M. K., Levi, V., Jaurez-Salinas, H., Barton, R. A., & Jacobson, E. L. (1980) *Cancer Res. 40*, 1797–1802.

Jaurez-Salinas, H., Sims, J. L., & Jacobson, M. K. (1979) *Nature (London) 282*, 740–741.

Kato, T., Berger, S. J., Carter, J. A., & Lowry, O. H. (1973) *Anal. Biochem. 53*, 86–97.

Mendelsohn, J. S., Skinner, S. A., & Kornfeld, S. (1971) *J. Clin. Invest. 50*, 818–826.

Miller, E. G. (1977) *Fed. Proc., Fed. Am. Soc. Exp. Biol. 36 (No. 3)*, 3349A.

Oikawa, A., Tohda, H., Kanai, M., Miwa, M., & Sugimura, T. (1980) *Biochem. Biophys. Res. Commun. 97*, 1311–1316.

Petzold, S. J., Booth, B. A., Leimback, G. A., & Berger, N. A. (1981) *Biochemistry 20*, 7075–7081.

Rankin, P. W., Jacobson, M. K., Mitchell, V. R., & Busbee, D. L. (1980) *Cancer Res. 40*, 1803–1807.

Sims, J. L., Jaurez-Salinas, H., & Jacobson, M. K. (1980) *Anal. Biochem. 106*, 296–306.

Sims, J. L., Berger, S. J., & Berger, N. A. (1981) *J. Supramol. Struct. Cell. Biochem. 16*, 281–288.

Steady-State Fluorescence Polarization of Dansylcadaverine–Fibrinogen: Evidence for Flexibility†

Roy R. Hantgan

ABSTRACT: The conformation of fibrinogen in solution has been investigated by steady-state fluorescence polarization measurements. Factor XIIIa has been employed to enzymatically incorporate 1–6 mol of dansylcadaverine/mol of fibrinogen into a specific glutamine residue near the carboxy terminus of the γ chain and up to two sites on the α chain. The fluorescence emission maximum of the labeled protein is shifted to 495 nm (from 538 nm for the fluorophore in solution) and the intensity substantially enhanced, indicating the covalently linked dansyl groups residue in a hydrophobic environment in the interior of the protein. This covalent modification does not interfere with the formation of fibrin, following thrombin activation. Steady-state fluorescence polarization measurements were carried out as a function of temperature and in high viscosity solvents. The fluorescent lifetime of dansylcadaverine–fibrinogen was determined by a phase shift technique. Analysis of the data by the Perrin–Weber treatment yields a rotational relaxation time of 160 ns, considerably faster than any realistic hydrodynamic model of fibrinogen would predict. The results are discussed in terms of segmental flexibility.

Fibrinogen is a soluble plasma protein of molecular weight 340 000 comprised of three pairs of polypeptide chains ($A\alpha$, $B\beta$, and γ) which are covalently linked by numerous disulfide bonds. Although the primary structure of fibrinogen has been determined (Henschen & Lottspeich, 1980; Doolittle, 1980), molecular details of its three-dimensional structure are still under active investigation. Hall & Slayter (1959) proposed a trinodular structure for fibrinogen, based on electron micrographs of shadowed specimens, in which two outer spheres 6–7 nm in diameter are connected by thin threads to a smaller central nodule (5-nm diameter). Hydrodynamic data indicate that fibrinogen can be treated as a long prolate ellipsoid, although uncertainties concerning the degree of hydration and contributions of the less ordered portions of the α chains

† From the Department of Biochemistry and Nutrition, University of North Carolina, Chapel Hill, North Carolina 27514. *Received September 25, 1981.* This work was supported by Grant-in-Aid 79 846 of the American Heart Association, with funds contributed in part by the North Carolina Heart Association and by National Institutes of Health Grant HL20319.

0006-2960/82/0421-1821$01.25/0

complicate matters (Doolittle, 1973). The fragments derived from proteolytic cleavage of fibrinogen correspond, approximately, to the dimensions of the nodules of the Hall and Slayter model (Marder et al., 1969; Fowler et al., 1980). Recently, the trinodular structure has been confirmed by high-resolution electron micrographs of both shadowed and negatively stained specimens (Fowler & Erickson, 1979). Using the amino acid sequence data and a helix prediction scheme, Doolittle and colleagues have postulated that the three polypeptide chains which join these globular domains are arranged as coiled coils (Doolittle et al., 1978). Electron microscopic evidence for further resolution of the basic Hall and Slayter model into a multinodular structure has recently been presented (Weisel et al., 1981; Williams, 1981).

One of the most intriguing aspects of the conformation of fibrinogen is the possibility that it is flexible; one of the nodules of this multidomain structure could bend or twist independently, i.e., not coupled to overall rotational motions of the rest of the molecule. Experimental evidence supporting flexibility was first presented by Johnson & Mihalyi (1965); their measurement of a rotational relaxation time of 195 ns for chemically labeled dansylfibrinogen by a steady-state fluorescence polarization technique indicated a considerably faster rate of molecular rotation than would be expected for a molecule the size and shape of fibrinogen. Recent electron microscopic studies have demonstrated a significant fraction of bent, i.e., nonlinear, molecules in both shadowed and negatively stained specimens (Fowler & Erickson, 1979), indicating some degree of flexibility. Electron microscopic examination of trimer complexes, composed of one fibrin monomer molecule noncovalently bound to an unactivated, cross-linked fibrinogen dimer, reveals that the outer, D domains of the monomer are frequently bent away from the central, E nodule of the dimer (Fowler et al., 1981b). Weisel et al. (1981) have also presented electron microscopic evidence favoring a moderate degree of flexing for the fibrinogen structure. Additional electron microscopic, hydrodynamic, and immunochemical data support the concept of a flexible fibrinogen conformation (Hudry-Clergeon et al., 1975; Marguerie, 1979; Serrallach et al., 1979; Fair et al., 1981).

In this study, factor XIIIa, a transglutaminase purified from normal human plasma (McDonagh & McDonagh, 1980), has been employed to catalyze the incorporation of the fluorophore dansylcadaverine into specific sites on fibrinogen. The physiological function of factor XIIIa is to stabilize the fibrin clot by catalyzing the formation of peptide bonds between specific lysine donor and glutamine acceptor sites on the γ and α chains of fibrin (Lorand et al., 1968a; Pisano et al., 1969). Dansylcadaverine acts as an inhibitor of the fibrin cross-linking reaction (Lorand et al., 1968b) and can form an isopeptide bond with the glutamine donor sites at residues 405 of the γ chain and up to three glutamines near the carboxy terminal of the α chain (residues 237, 328, and 266) (Takagi & Doolittle, 1975; Cottrell et al., 1979; Doolittle et al., 1979). In fibrin, dansylcadaverine is incorporated more rapidly into the γ chains than to the α-chain acceptor sites; in fibrinogen the overall rate of incorporation of dansylcadaverine is slower than for fibrin, and there is evidence that not all the acceptor residues are identical with those in fibrin (Lorand et al., 1966, 1972). However, the γ-chain acceptor site on fibrinogen is known to reside near the carboxy terminus, at the distal end of the outer D domain (Chen & Doolittle, 1971; Kanaide & Shainoff, 1975; Fowler et al., 1981a).

The rotational relaxation time, which can be determined from measurements of the steady-state fluorescence polarization as a function of temperature and solvent viscosity (Perrin, 1934), is a sensitive function of the size and shape of a macromolecule. Conversely, if the molecular dimensions of a protein are reasonably well-defined, this measurement can be used as a probe of molecular flexibility (Weber, 1953; Steiner & McAlister, 1957; Chen et al., 1969). Although the fluorescent lifetime of the intrinsic tryptophan residues is too short to observe depolarization with a molecule as large as fibrinogen, the longer lifetime of dansyl protein conjugates is suitable for this technique (Steiner & McAlister, 1957), and the emission and polarization properties of chemically dansylated fibrinogen have been extensively studied (Johnson & Mihalyi, 1965; Mihalyi & Albert, 1971a,b). However, the specificity of labeling which is possible by using factor XIIIa catalyzed incorporation of dansylcadaverine into the γ and α chains of fibrinogen offers unique advantages. The location of the γ-chain acceptor site is well-defined, and the presence of one dansylcadaverine molecule per γ chain and on a limited number of α-chain sites does not impede the fibrin formation process (Fowler et al., 1981a). The results obtained in this study provide additional evidence in support of a flexible structure for fibrinogen in solution. A preliminary report of this work has appeared in abstract form (Hantgan, 1981).

Experimental Procedures

Materials. Human fibrinogen (grade L, Kabi, Stockholm, Sweden) was dissolved in 0.3 M NaCl and dialyzed at 4 °C for 18 h in order to remove free calcium. The solution was centrifuged at 30000*g* for 20 min, divided into aliquots, and stored at −70 °C. Clottability was approximately 93% by the method of Laki & Lorand (1948). Fibrinogen concentrations were determined from the absorbance at 280 nm by using a specific extinction coefficient of 1.6 mL^{-1} mg^{-1} cm (Carr & Hermans, 1978). Purified human thrombin was kindly provided by Dr. J. W. Fenton. Factor XIII was a gift from Dr. J. McDonagh and was activated with thrombin and assayed by published procedures (McDonagh & McDonagh, 1980). The thrombin inhibitor Val-Ile-Pro-Arg-chloromethyl ketone (Kettner & Shaw, 1977) was generously provided by Dr. E. Shaw. Hirudin (grade IV) and monodansylcadaverine were purchased from Sigma. Trasylol 10000 KIU/mL (Kallikreinin international units) was purchased from Mobay Chemical Corp.

Preparation of Dansylcadaverine–Fibrinogen. The basic procedure for factor XIIIa catalyzed incorporation of dansylcadaverine into fibrinogen has been previously described (Fowler et al., 1981a). In this study that procedure was modified, as follows, to favor the formation of monomeric dansylcadaverine–fibrinogen. Factor XIII was activated in 0.5 M NaCl, 0.05 M Tris, and 0.005 M $CaCl_2$, pH 7.4, at 37 °C with 1.5 units/mL thrombin for 30 min, and then the thrombin was inhibited with hirudin at 30 units/mL; fibrinogen and dansylcadaverine were next added to final concentrations of 5×10^{-6} and 1.5×10^{-3} M, respectively. The time of the labeling reaction was varied from 15 to 180 min and the factor XIIIa concentration from 0.01 to 0.08 mg/mL in order to produce derivatives with varying degrees of fluorescent labeling. The reaction mixtures were concentrated 6-fold by dialysis vs. solid PEG 14000, and then chromatographic separations were performed on a 2.6 × 85 cm Sepharose 4B column eluted with 0.1 M NaCl, 0.05 M Tris, pH 7.4, and 10 KIU/mL Trasylol at 15 mL/h. Elution was followed by the absorbance at 280 nm and the fluorescence at 500 nm (365 nm excitation). Fractions of monomeric dansylcadaverine–fibrinogen were pooled and dialyzed vs. 0.3 M NaCl and 10 KIU/mL Trasylol at 4 °C for 18 h and then

frozen and stored in aliquots at −70 °C. Thawed samples were dialyzed vs. the appropriate buffer for 18 h at 4 °C and then centrifuged for 30 min at 30000*g* prior to spectroscopic measurements.

Polyacrylamide Gel Electrophoresis. Samples were reduced by 1% dithiothreitol/1% sodium dodecyl sulfate at 100 °C for 5 min prior to electrophoresis on 7% gels in the presence of 0.1% sodium dodecyl sulfate. Polyacrylamide gel electrophoresis of reduced fibrinogen under these conditions allows the separation of the three constituent polypeptide chains of fibrinogen (molecular weights: Aα, 70000; Bβ, 58000; γ, 47000). For quantitation of the location of the fluorescent label(s), the gels were photographed with ultraviolet light excitation by using a yellow filter (Kodak no. 15) and Tri-X (ASA 400) film. The use of exposure times < 10 s kept the response of the film in the linear range (Pulleybank et al., 1977). The negatives were then scanned with a Joyce-Loebl microdensitometer and the areas of the fluorescent peaks determined by treating the peaks as Gaussian (i.e., the area is proportional to the peak height × width at half-height). For a given gel, the ratio of areas of the fluorescent peaks was independent of exposure time, confirming the validity of the quantitation. The gels were then stained with Coomassie blue and the molecular weights of the bands determined from the mobility of protein standards run with each set of gels, as well as by comparison with unlabeled fibrinogen samples.

Determination of the Degree of Dansylcadaverine Incorporation. Samples of dansylcadaverine–fibrinogen were dialyzed vs. 6 M guanidine hydrochloride and 0.05 M Tris, pH 8.0, for 18 h at room temperature, and the fluorescence spectra were recorded at room temperature with a Perkin-Elmer MPF-3 spectrofluorometer equipped with a Canrad-Hanovia 200-W xenon–mercury arc lamp and Electro Powerpacs Corp. Model 114B lamp power supply. Excitation was at 365 nm, for which dansylcadaverine–fibrinogen was found to exhibit a broad emission maximum centered at approximately 530 nm under denaturing conditions. When the observed intensity was compared to that of dansylcadaverine standards (λ_{max} 538 nm), it was possible to quantitate the extent of fluorescent labeling, in a manner similar to other published assay procedures (Lorand et al., 1969). The concentration of fibrinogen was determined from the absorbance at 280 nm by using the extinction coefficient of (unlabeled) fibrinogen (Carr & Hermans, 1978), as the dansyl chromophore contributed very little to the absorbance at 280 nm, under these conditions of minimal labeling (Mihalyi & Albert, 1971a).

Light Scattering. The apparatus and procedures for measurements of the intensity of light scattered at right angles to a solution have been previously described (Hantgan & Hermans, 1979). In this study, intensity vs. time measurements were employed to compare the rate and extent of fiber formation (following addition of non-rate-limiting thrombin concentrations) of dansylcadaverine–fibrinogen to the native protein. Fibrinogen concentrations of 0.01–0.02 mg/mL in 0.1 M NaCl, 0.05 M Tris, and 10 KIU/mL Trasylol, pH 7.4, were examined.

Clottability. The amount of clottable dansylcadaverine–fibrinogen was determined by the method of Laki & Lorand (1948).

Fluorescence Polarization Measurements. For polarization measurements, a Perkin-Elmer MPF-3 spectrofluorometer was used with a polarization module consisting of an Oriel near-UV–visible linear excitation polarizer fixed in the vertical position and an Oriel visible linear emission polarizer which was set either parallel or perpendicular to the excitation polarizer. The use of a multiwave plate depolarizer between the analyzer and detector eliminated the need for correction of differential sensitivity of the optical system to vertically and horizontally polarized light (Lentz et al., 1978). To obtain the polarization spectra, the excitation wavelength was set at 365 nm and the emission scanned from 480 to 510 nm with the emission polaroid first parallel and then perpendicular to the excitation polaroid. This sequence was repeated at least 3 times at each temperature and the value of the intensities ($I_\parallel$ and $I_\perp$) at λ_{max} (495 nm) measured from the scans. The value of the polarization, P, was calculated from each pair of intensities, according to eq 1, and the results were averaged.

$$P = I_\parallel - I_\perp/(I_\parallel + I_\perp) \quad (1)$$

The standard deviation of the data was typically ±0.003 polarization unit. Polarization measurements were made as a function of temperature, in steps of 5 °C, from 5 to 40 °C in a typical experiment. The cell temperature was maintained at ±0.05 °C with a Haake D3-G circulating water bath and a thermostated cell block with a magnetic stirring attachment. The temperature was measured with a Yellow Springs Instrument Model 702A thermistor probe and a Digitech Digital Model 5810 thermometer (readings could be made to ±0.01 °C). At temperatures less than 20 °C, the cell compartment was flushed with dry N_2 in order to avoid condensation problems. Data at high solvent viscosities were obtained by measuring the polarization at 0 °C in 60% and 76% glycerol, 0.1 M NaCl, 0.05 M sodium phosphate, pH 7.4, and 54% sucrose, 0.1 M NaCl, 0.05 M sodium phosphate, pH 7.4. The concentrations of sucrose and glycerol used to obtain data at high viscosities were determined from measurements of the refractive index of the solutions at 20 °C, with a Bausch & Lomb refractometer.

Fluorescence Lifetime Measurements. Lifetime measurements were carried out on an SLM 4800 spectrofluorometer by a phase shift technique (Lakowicz et al., 1979). The phase and modulation differences were determined at 6, 18, and 30 MHz by using a KV389 filter (Schott Optical Glass) to prevent exciting light from reaching the detector. Light scattered from a glycogen solution provided a zero lifetime reference standard. Various regions of the emission spectrum were examined with a KV550 filter (Schott Optical Glass) to isolate the long wavelength region, and 505- and 520-nm narrow band pass filters as well. The data obtained exhibited no dependence on the wavelength of emission; therefore the results were averaged, and this value was used as the fluorescent lifetime.

Results

Properties of Dansylcadaverine–Fibrinogen. The data presented in Figures 1–2 describe the purification and characterization of a (typical) preparation of dansylcadaverine–fibrinogen (in this case, obtained after a 90-min reaction period at 0.045 mg/mL factor XIIIa). As the elution profile in Figure 1 demonstrates, two fluorescent macromolecular species result from this preparation. The earliest eluting peak has been shown, by polyacrylamide gel electrophoresis and negative staining electron microscopy (Fowler et al., 1981a), to be dimeric fibrinogen, in which two molecules are covalently joined end-to-end through their γ-chain cross-link donor–acceptor sites present on the outer D domains of this multinodular protein. The major peak contains dansylcadaverine-labeled monomeric fibrinogen. The polyacrylamide gel shown in Figure 1 indicates label has been incorporated into both the γ- and α-chain acceptor sites of fibrinogen; this is consistent with results published earlier (Lorand et al., 1972). Quan-

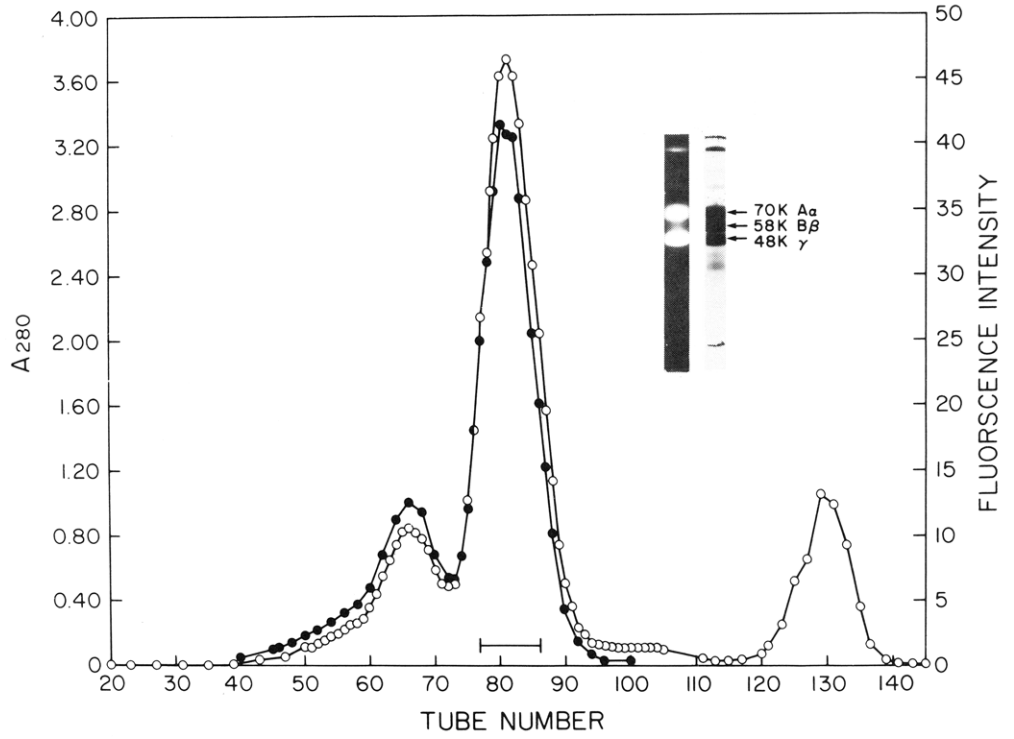

FIGURE 1: Chromatography of dansylcadaverine–fibrinogen reaction mixture on a Sepharose 4B (2.6 × 85 cm) column. The elution profile was followed by the absorbance at 280 nm (○) and the fluorescence at 500 nm (excitation wavelength 365 nm) (●). The inset shows the electrophoretic pattern in 1% $NaDodSO_4$ of reduced samples of the major peak, photographed with UV illumination (left) prior to staining and stained with Coomassie blue (right).

titative gel scans have allowed a determination of the ratio of label in the γ to the α chain, 1.3 ± 0.1 in this preparation. By measurement of the fluorescent intensity of a known concentration of this derivative under denaturing conditions, where the chromophore is fully exposed to the solvent (see Experimental Procedures and Figure 2), and comparison of its intensity to dansylcadaverine standards in the same solvent, it has been demonstrated that this derivative contains 2.1 mol of dansylcadaverine/mol of fibrinogen, therefore about 1.2 molecules/γ chain and 0.9 molecules/α chain of fibrinogen.

Clottability measurements have shown that 93% of the labeled protein forms a clot, upon thrombin activation. Thus the clottability is unchanged from that of the unlabeled (Kabi) fibrinogen starting material. All the dansylcadaverine–fibrinogen derivatives were examined with a sensitive light-scattering kinetic assay which measures the rate and extent of fiber formation under physiological buffer conditions (Hantgan & Hermans, 1979). The data obtained for each derivative demonstrated the same two-step reaction sequence of protofibril growth followed by lateral association of protofibrils to form fibrin, which has been established for the native protein. Incorporation of 1 mol of dansylcadaverine/mol of fibrinogen did not alter the initial polymerization step but did result in slower fiber growth and an increased fiber thickness (approximately twice the control values). Derivatives with 2–3 mol of dansylcadaverine/mol of fibrinogen showed the same pattern of increased fiber thickness, although quantitative variations which did not appear correlated with the degree of labeling were found. Derivatives containing 3–6 mol of dansylcadaverine/mol of fibrinogen were found to initiate lateral association after a shorter protofibril growth time. At 6 mol of dansylcadaverine/mol of fibrinogen, the final fiber thickness was approximately equal to the control values. These observations confirm the results of previous investigators who have shown that dansylcadaverine incorporation does not interfere with fibrin formation (Lorand et al., 1968b) and that dansylcadaverine labeled fibrinogen dimers from normal cross-banded fibrin following thrombin activation, as judged by negatively stained electron micrographs (Fowler et al., 1981a).

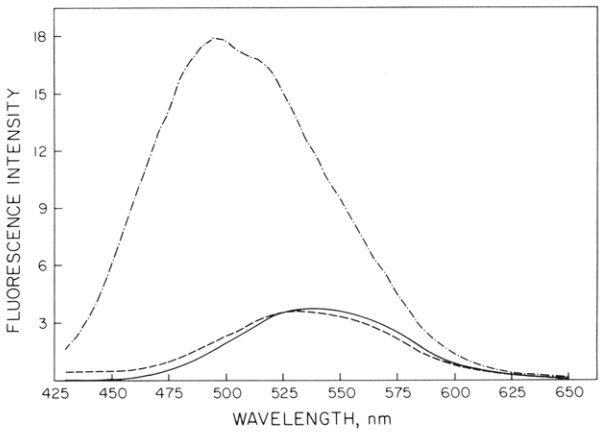

FIGURE 2: Fluorescence emission spectra (uncorrected, λ_{ex} 365 nm) of dansylcadaverine–fibrinogen (1.0×10^{-6} M) (- - -) in 0.1 M NaCl and 0.05 M Tris, pH 7.4, and in 6 M guanidine hydrochloride and 0.05 M Tris, pH 8.0 (- - -). The solid line represents the emission of dansylcadaverine (2.2×10^{-6} M) in the latter solvent.

At a fixed factor XIIIa concentration (0.045 mg/mL), reaction times of 15 min have yielded derivatives containing 1 mol of dansylcadaverine/mol of fibrinogen (with approximately equal incorporation into the γ and α chains), whereas increased reaction times resulted in greater incorporation. At 180-min reaction, derivatives containing 3 mol of dansylcadaverine/mol of fibrinogen were obtained; 2 mol/mol of γ chain and 1 mol/mol of α chain were incorporated. A preparation carried out at 0.08 mg/mL factor XIIIa for 180 min resulted in the incorporation of 5.8 mol of dansylcadaverine/mol of fibrinogen, although some α-chain degradation resulted, making a quantitative determination of the location of the

labeling sites uncertain.

Fluorescence Emission Spectra. The (uncorrected) fluorescence emission spectrum of dansylcadaverine–fibrinogen (Figure 2; λ_{ex} 365 nm) exhibits a maximum at 495 nm and a shoulder at approximately 520 nm. By comparison, the emission spectrum recorded under denaturing conditions, 6 M guanidine hydrochloride and 0.05 M Tris, pH 8.0, shows a 5-fold decreased intensity and broad maximum centered at about 530 nm. The emission spectrum of dansylcadaverine–fibrinogen under denaturing conditions is very similar to that obtained with the free ligand, dansylcadaverine, in either pH 7.4 buffer or concentrated guanidine hydrochloride solutions (λ_{max} 538 nm). A similar change in the emission characteristics of dansylcadaverine can be demonstrated in the presence of increasing ethanol concentrations. In absolute ethanol, dansylcadaverine displayed a 20-fold enhanced emission, with λ_{max} 500 nm. Similar results have been reported for other naphthalenesulfonate dyes in alcohol solutions (McClure & Edelman, 1966).

Steady-State Fluorescence Polarization. The polarization data, obtained as a function of temperature and solvent viscosity, were analyzed by a Perrin plot which is based on the equation (Perrin, 1934; Weber, 1953)

$$(1/P - 1/3)/(1/P_0 - 1/3) = 1 + \frac{k\tau}{V}\left(\frac{T}{\eta}\right) \qquad (2)$$

In a Perrin plot, the function $(1/P - 1/3)$ is plotted vs. the temperature to viscosity ratio (T/η). The data were analyzed by a linear regression procedure. The intercept of this plot, $(1/P_0 - 1/3)$, determines P_0, the value of the polarization measured in the absence of molecular motion, i.e., $T/\eta = 0$. This parameter was also determined directly by measurements in concentrated glycerol or sucrose solutions at 0 °C. The ratio of slope to intercept in a Perrin plot determines $k\tau/V$, the ratio of the fluorescent lifetime τ to the molecular volume V multiplied by the Boltzmann constant, k, which can be used to calculate the rotational relaxation time (ρ) according to the following equation, provided the fluorescent lifetime is also known:

$$\rho = 3\eta V/(kT) \qquad (3)$$

Although the theory was originally derived by Perrin (1934) for spherical molecules, Weber (1953) has extended this treatment to prolate ellipsoids of revolution and shown that the measured ρ corresponds to ρ_h, the harmonic mean of the rotational relaxation times about the principal axes of the ellipsoid, and V corresponds to the hydrated volume of the ellipsoid.

The fluorescent lifetime of dansylcadaverine covalently attached to fibrinogen was measured with a preparation containing 2.9 mol of dansylcadaverine/mol of fibrinogen in 0.10 M NaCl and 0.05 M Tris, pH 7.4, 20 °C. Values of 14.8 ± 2.9 and 15.0 ± 2.3 ns were obtained in two separate experiments by collecting all emitted light and averaging the lifetimes obtained by the phase and modulation modes at frequencies of 6, 18, and 30 MHz. (Dansylcadaverine free in solution exhibited a 3-ns lifetime.) The precision of the data is insufficient to resolve these lifetimes into more than one component, although the possibility of heterogeneity in the lifetime cannot be rigorously excluded. The lifetime was measured in three selected regions of the emission spectrum to further pursue this question. By use of 505- and 520-nm narrow band pass filters, regions near the peak and small shoulder, respectively, were examined; lifetimes of 14.3 ± 2.9 and 14.1 ± 3.6 ns resulted. By isolation of the long wavelength region with a 550-nm cutoff filter, a value of 14.5 ± 1.9 ns was obtained. As the lifetime data showed no dependence on wavelength, the results of measurements in which all emitted light was collected were averaged, and a value of 14.9 ± 2.5 ns was used in subsequent calculations. This value is in good agreement with literature values for chemically dansylated protein conjugates, including dansylcadaverine–fibrinogen (Steiner & MacAlister, 1957; Mihalyi & Albert, 1971a).

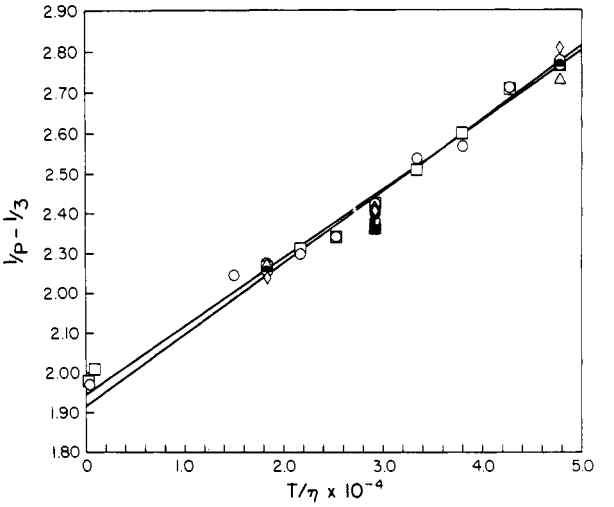

FIGURE 3: Perrin plot of the dependence of the polarization vs. temperature/viscosity for dansylcadaverine–fibrinogen preparations labeled with 1.1 (○) and 1.2 (□) mol of dansylcadaverine/mol of fibrinogen. Solutions contained 0.1 M NaCl and 10 KIU/mL Trasylol and were buffered as indicated: (◇) 0.05 M Tris, pH 8.5; (○) 0.05 M Tris, pH 7.4; (●) 0.05 M phosphate, pH 7.4; (△) 0.05 M phosphate, pH 6.5. The solid symbols denote measurements made at the end of the temperature series, after returning to 20 °C. The symbol ◐ indicates an average of points obtained at 20 °C with dansylcadaverine–fibrinogen concentrations ranging from 0.12 to 1.92 mg/mL. The symbols on the left ordinate denote data obtained in high-viscosity solvents at 0 °C (60% and 76% glycerol). The solid lines represent independent least-squares fits of the data for the two preparations to the Perrin equation.

The data in Figure 3 have been obtained with two dansylcadaverine–fibrinogen preparations, containing 1.1 and 1.2 mol of dansylcadaverine/mol of fibrinogen. The data verify that the linear fit to the Perrin equation is valid ($r^2 > 0.98$) and that the limiting polarization obtained in high viscosity solvents is in good agreement with the intercept obtained from extrapolation of the linear regression line. The solid points represent measurements made after the sample had been examined at temperatures from 0 to 40 °C and returned to 20 °C. The changes in polarization were found to be reversible, provided the temperature was not raised above 40 °C, precipitation occurring from 45 to 50 °C. Points obtained at 20 °C and at protein concentrations from 0.12 to 1.92 mg/mL showed no evidence of concentration dependence. Also points obtained at 5, 20, and 40 °C in solutions buffered with phosphate at pH 6.5 and 7.4 and Tris at pH 7.4 and 8.5 showed no evidence of pH-dependent polarization changes over the range examined. The rotational relaxation times obtained for the two independent preparations agreed, within experimental error; this indicates that the dansylcadaverine labeling procedure yields a reproducible derivative. As these data confirm the validity of the experimental procedures, the effect of varying the degree of labeling can be considered next.

The data in Figure 4 were obtained with derivatives containing 1.1, 2.1, 2.9, and 5.8 mol of dansylcadaverine/mol of fibrinogen. Here again, a linear fit to the Perrin equation (eq 2) is obtained with all derivatives. Although there are small differences in the slopes and intercepts of the linear regression

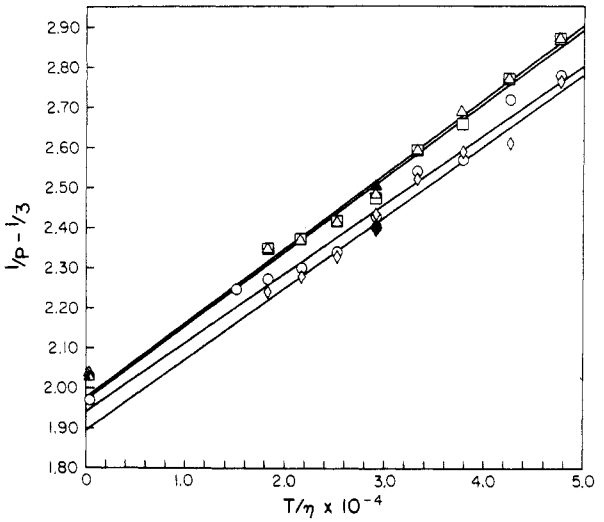

FIGURE 4: Perrin plot of the dependence of the polarization vs. temperature/viscosity for dansylcadaverine–fibrinogen preparations labeled with 1.1 (○), 2.1 (◇), 2.9 (□), and 5.8 (△) mol of dansylcadaverine/mol of fibrinogen. Data were obtained in 0.1 M NaCl, 0.05 M Tris, pH 7.4, and 10 KIU/mL Trasylol. The solid symbols denote measurements made at the end of the temperature series, after returning to 20 °C. The symbols on the left ordinate denote data obtained in high-viscosity solvents at 0 °C [54% sucrose (▲) and 76% glycerol (△, ○)].

Table I: Summary of Polarization Parameters

degree of labeling (mol of DC/mol of fibrinogen)	rotational relaxation time (ns) at 20 °C	limiting polarization ($1/P_0 - 1/3$)
1.1	172	1.970
1.2	163	1.915
2.1	165	1.895
2.1 (0.5 M NaCl)	159	1.888
2.7	155	2.023
2.7	143	1.896
2.9	164	1.973
2.9 (0.005 M $CaCl_2$)	145	1.904
5.8	166	1.950
5.8	164	1.976
	160 ± 9[a]	1.939 ± 0.046[a]

limiting polarization in high-viscosity solvents:
(a) 54% sucrose, 0 °C, 2.034 ± 0.031
(b) 76% glycerol, 0 °C, 2.011 ± 0.046
(c) fibrin gel, 20 °C, 1.90 ± 0.12

[a] Average value ± SD.

analyses, there appears to be no dependence of ρ or P_0 on the degree of labeling. Table I summarizes the rotational relaxation times obtained for all preparations examined in this study and shows that an average rotational relaxation time of 160 ± 9 ns is obtained. The rotational relaxation time was not affected by increased ionic strength (0.5 M NaCl) or the presence of calcium ions in the buffer, conditions which can influence the fibrin assembly process (Hantgan & Hermans, 1979).

Table I also compares the (averaged) P_0 values calculated from the intercepts of the fitted lines to the limiting polarization measured in high-viscosity solvents. The measured P_0 values are slightly higher than the extrapolated values, as was observed for chemically dansylated fibrinogen (Johnson & Mihalyi, 1965). The change in polarization (at constant temperature) which occurs upon thrombin activation of dansylcadaverine–fibrinogen and the subsequent formation of a fibrin gel has also been investigated, as another experimental approach to determine the polarization under conditions of minimum molecular motion. The value cited for the fibrin gel in Table I is an average of points obtained by clotting fibrinogen at 20 °C in 0.1 M NaCl, 0.05 M Tris, and 10 KIU/mL Trasylol, pH 7.4, at fibrinogen concentrations from 0.05 to 0.30 mg/mL. This value is 20% higher than that observed at the same temperature for solutions of dansylcadaverine–fibrinogen. Although these points display less precision than the solution values, the polarization obtained with fibrin gels does agree with the parameters obtained in high viscosity solvents.

Table II: Calculated Hydrodynamic Parameters

shape	dimensions	distribution of probe	rotational relaxation time (ns)
sphere	diameter = 9.2 nm	random	300
prolate ellipsoid	42 × 4.2 nm	random	555
prolate ellipsoid	$b/a \rightarrow 0$	random	600
prolate ellipsoid	42 × 4.2 nm	parallel to long axis	4000
prolate ellipsoid	42 × 4.2 nm	parallel to short axis	388

Discussion

In this study a rotational relaxation time (ρ) of 160 ns has been determined by the technique of steady-state fluorescence polarization with fibrinogen covalently labeled at specific glutamine residues by dansylcadaverine. For assessment of the significance of the measured ρ for dansylcadaverine–fibrinogen, values of ρ have been calculated for reasonable spherical and ellipsoidal models of the fibrinogen molecule and are summarized in Table II.

Calculated Hydrodynamic Parameters. (*A*) *Sphere.* When a partial specific volume of 0.715 mL/g for fibrinogen (Doolittle, 1980) and a molecular weight of 340 000 are used, a (anhydrous) molecular volume (V) of 4.04×10^{-19} cm^3 results. This corresponds to a sphere of diameter 9.2×10^{-7} cm. When Stokes' law is used, a rotational frictional coefficient (f_R) may be calculated.

$$f_R = 6\eta V \quad (4)$$

The rotational relaxation time is then calculated according to (Weber, 1953)

$$\rho = f_R/(2kT) \quad (5)$$

This gives ρ = 300 ns for the spherical model.

(*B*) *Ellipsoid.* An ellipsoid of revolution is characterized by a long semiaxis (a) and two equivalent short semiaxes (b). Choosing an axial ratio of 10, which approximately fits the dimensions of fibrinogen observed by electron microscopy (Fowler & Erickson, 1979), and the molecular volume calculated above, dimensions of $2a = 4.2 \times 10^{-6}$ cm and $2b = 4.2 \times 10^{-7}$ cm result.

Depolarization of the fluorescence emitted from a fluorophore attached in a wide variety of points to such a prolate ellipsoid results from rotation about both the long and short axes. Two frictional coefficients or two rotational relaxation times are needed to characterize such an ellipsoid; steady-state fluorescence polarization measurements yield the harmonic mean of these times. Equations were derived by Perrin (1934) and Weber (1953) and have been cast in a convenient form by Cantor & Schimmel (1980). A detailed treatment of the equations employed to calculate the parameters in Table II follows in the Appendix. Values of ρ are cited in Table II for

an axial ratio of 10 as well as the value obtained in the limit of an infinitely long prolate ellipsoid.

As the data presented earlier have shown that dansylcadaverine has been incorporated into a limited number of acceptor sites in the γ and α chains of fibrinogen, the assumption of random orientation of the probe, with respect to the long axis of the ellipsoid, may not be strictly valid. Following a treatment described by Weber (1953), the consequences of nonrandom probe orientation can be ascertained. First, consider the case in which the probe is preferentially aligned parallel to the long axis of the ellipsoid. In this case, the (less hindered) rotation about the long axis will not reorient the probe and thus will not cause depolarization of fluorescence (Weber, 1953; Tao, 1969). ρ is then determined by rotation about the short axes only, and a value of 4000 ns is calculated. If the probe were preferentially oriented parallel to one short axis, only rotations about the long axis and the other short axis would contribute to observed depolarization. For this case ρ = 388 ns for an axial ratio of 10, and a limiting value of 400 ns is predicted.

The value of ρ determined in this study is considerably faster than ρ calculated for the spherical and ellipsoidal models cited in Table II and is only slightly faster (20%) than that previously reported for steady-state fluorescence polarization measurements with chemically dansylated fibrinogen (195 ns) (Johnson & Mihalyi, 1965). (The difference between these rotational relaxation times may be due to the consequences of specific vs. random labeling of the macromolecule, as previously discussed, or may reflect minor structural changes induced by the labeling procedures.) This result indicates that the molecular unit whose motion causes the observed depolarization is smaller than the entire fibrinogen molecule. There are two possible explanations for this decreased ρ. Either the dansylcadaverine probe is not rigidly attached to the protein or the macromolecule itself is not rigid but possesses modes of internal flexibility. These two possibilities will be considered in detail in the sections which follow.

Probe Rotation. According to theory (Perrin, 1934; Weber, 1953; Steiner & MacAlister, 1957), the ideal fluorescent probe should be rigidly attached to a wide variety of locations on the macromolecule, so that no single orientation of the fluorophore dominates the depolarization. In practice, specificity of labeling can be useful in order to minimize contributions due to free rotation of a solvent-exposed fluorescent probe. Although the factor XIIIa catalyzed dansylcadaverine incorporation procedure did not yield derivatives with label only on the γ chain of the outer D domains of fibrinogen, or exclusively on the α chain, the limited number of sites labeled does offer an advantage over the chemical dansylation procedure which is likely to label any lysine residue on the surface of the protein. [The previously reported study of steady-state polarization of fibrinogen (Johnson & Mihalyi, 1965), for example, employed a chemically dansylated protein containing 11–13 mol of dansyl/mol of fibrinogen.] However, the fluorophore in these dansylcadaverine derivatives is attached to the polypeptide chain of the protein through a 12–15-Å-long connector, so that the problem of probe rotation still must be considered. Spectroscopic evidence which addresses this point is presented in the following paragraphs.

In this study, dansylcadaverine derivatives containing one to six molecules of fluorophore per fibrinogen molecule have been examined. The results obtained show no dependence of the rotational relaxation time or the value of P_0 on the degree of labeling. In addition, the P_0 values determined by extrapolation of the polarization to $T/\eta = 0$ agree, within experimental error, with the values measured directly for the dansylcadaverine–fibrinogen derivatives in high viscosity solvents at 0 °C. Furthermore, the polarization measured with dansylcadaverine–fibrin gels is significantly higher than that observed for solutions of dansylcadaverine and agrees with P_0 values determined in high viscosity solvents; i.e., immobilization of dansylcadaverine–fibrinogen either by gelation or by the combination of low temperature and high solvent viscosity leads to the same increase in polarization, consistent with the restriction of molecular rotation under these circumstances. These values also agree with published values for P_0 measured with low molecular weight compounds containing the dansyl moiety (Wahl & Weber, 1967). Free rotation of the fluorophore would result in a higher value of P_0 in high viscosity solvents than would be predicted from the Perrin equation (eq 2) (Chen et al., 1969). These results verify the assumption that probe motion contributes little, if anything, to the observed fluorescence depolarization.

The fluorescence emission spectrum shows a shift in the wavelength of maximum emission (λ_{max}) from 538 (free dansylcadaverine) to 495 nm upon coupling to the protein. Similar blue shifts have been reported for a variety of naphthalenesulfonate dyes bound to proteins or in organic solvents (Stryer, 1965; McClure & Edelman, 1966; Lorand et al., 1971). The fluorescent lifetime data, examined across the emission peak, show a considerably longer lifetime for the protein-bound probe compared to dansylcadaverine in solution (15 vs. 3 ns). The emission is also significantly enhanced when the fluorophore is covalently bound to fibrinogen. These observations indicate that the dansyl fluorophore resides in a hydrophobic region of the protein, not exposed to the surrounding solvent. Disruption of the tertiary structure of the protein by guanidine hydrochloride results in a nearly complete exposure of the fluorophores to the solvent; λ_{max} shifts to 530 nm, and the intensity of emission is substantially reduced.

Polyacrylamide gel electrophoresis establishes that dansylcadaverine has been covalently coupled to up to two sites on the γ chains (one on each D domain) and up to four sites on the α chains, depending on the total degree of incorporation. Measurements of the extent and rate of gelation of dansylcadaverine–fibrinogen, following thrombin activation, verify that incorporation of dansylcadaverine does not seriously interfere with the function of fibrinogen. These observations confirm the results of other investigators (Lorand et al., 1968b; Fowler et al., 1981b) and raise a number of interesting questions about the relationship between the location of the γ chain acceptor site and the noncovalent contact sites responsible for maintaining the stability of the fibrin protofibril, an intermediate in fibrin formation (Fowler et al., 1981b). Although this region must be accessible to factor XIIIa in order to form the covalent cross-link, in the absence of direct structural information it is difficult to distinguish between the possibilities that, e.g., the dansyl moiety is buried in the interior of the D domain, as the fluorescent spectral data indicates, or the alternative explanations that the dansyl group either can move or is located some distance away from the specific residues which interact to form the noncovalent intermolecular contacts between the D domains of adjacent fibrin monomers in the protofibril.

Some experimental evidence supports the concept that large portions of the α chain, including the potential labeling sites, are mobile and freely exposed to water (Takagi & Doolittle, 1973). However, other data show that this region is not without structure (Mihalyi, 1981). The shoulder seen at 520 nm in the emission spectrum of dansylcadaverine may be due

to that small contribution from α-chain-attached probes, which if they are more exposed to solvent, would emit at a longer wavelength, more like the fluorophore free in solution. At the wavelength emission maximum, only 11% of the observed fluorescence intensity could be contributed by a solvent-exposed fluorophore; at the shoulder the contribution is estimated to be about 20% of the total signal. The rotational relaxation times measured at both 495 and 520 nm, with the most highly labeled derivative, were 166 and 148 ns, respectively. This represents only an 11% faster ρ in a region of the spectrum where contributions from the α-chain label would be greatest. In summary, ρ has been found to be independent of the degree of labeling and its low value not simply attributable to probe rotation.

Flexibility. The measured ρ is significantly less than that calculated for any hydrodynamic model of fibrinogen. The lowest value of ρ calculated, that for an anhydrous sphere, is nearly twice the observed value. Any added water of hydration would uniformly increase any of the calculated values. Although steady-state fluorescence polarization measurements must yield a mean of the rotational relaxation times involved, with possible contributions from segmental flexibility as well as overall macromolecular rotation, the data do provide strong support for the hypothesis that fibrinogen is not a rigid molecule but in fact can undergo bending or twisting motions in solution. These steady-state fluorescence polarization experiments do not define the site(s) of flexibility, but a consideration of the available structural data does provide a basis for speculation. Fibrinogen is clearly a multidomain protein, as a limited proteolytic cleavage yields globular fragments (D and E) which display thermal transitions corresponding to the two melting points seen in the intact molecule (Donovan & Mihalyi, 1974). Doolittle (1977) has used a helix prediction scheme and sequence data to postulate that the regions of polypeptide chain connecting the outer, D domain to the central E domain are arranged as coiled coils which are terminated at each end by cystine links in an arrangement referred to as the "disulfide swivel". Doolittle (1977) has suggested that these three stranded helices behave as coiled springs and are in part responsible for the elasticity of the fibrin gel. This suggests that the coiled-coil regions may be the site of molecular flexibility in fibrinogen. Alternatively, the disulfide rings which connect the globular to the helical regions of fibrinogen may be the site of flexibility. Segmental motion about a molecular hinge has been demonstrated in the case of the immunoglobin G molecule (Yguerabide et al., 1971).

Either description would also allow the possibility that the outer, D domains, which contain the γ-chain-linked dansylcadaverine, could rotate, over a limited range, independent of the central E domain. It is interesting to note that a sphere of diameter 6 nm, which corresponds to the dimensions of the D domain seen by negative staining electron microscopy as well as to the volume of an anhydrous protein of 100 000 molecular weight, would exhibit a rotational relaxation time of approximately 90 ns. The limiting value for a prolate ellipsoid of the same volume is 180 ns. These values are in the time range observed for the rotational relaxation time of dansylcadaverine–fibrinogen and further suggest that the independent rotation of D domain contributes to the observed depolarization.

The observation of molecular flexibility on the nanosecond time scale may be of interest on physiological as well as protein structural grounds. The fibrin gel is characterized by frequent network branchpoints (Hantgan & Hermans, 1979; Fowler et al., 1981b) in which one fiber must bend away from another fiber. Assembling such a network from inherently flexible molecules would offer a distinct structural advantage.

Acknowledgments

The expertise of David Barrow and Dr. Barry Lentz in obtaining the lifetime data is gratefully acknowledged. Special thanks are due to Drs. Jan McDonagh and Jan Hermans for stimulating discussions. I am especially grateful to Edward Nolan for his excellent technical assistance.

Appendix

A prolate ellipsoid of revolution can be characterized by a long semiaxis (a), a short semiaxis (b), and the ratio

$$p = b/a \tag{A1}$$

The rotational relaxation time for disorientation of the long axis, ρ_a, and of the short axis, ρ_b, is determined by the corresponding frictional coefficients (Cantor & Schimmel, 1980; Weber, 1953):

$$f_a = f_R 4(1 - p^2)/[3(2 - p^2 S)] \tag{A2a}$$

$$f_b = f_R 4(1 - p^4)/[3p^2[S(2 - p^2) - 2]] \tag{A2b}$$

in which

$$S = 2(1 - p^2)^{-1/2} \ln [[1 + (1 - p^2)^{1/2}]/p] \tag{A3}$$

In addition, f_R, the frictional coefficient, and the rotational relaxation time of the sphere of equivalent volume are given by

$$f_R = 6\eta V \tag{A4a}$$

$$\rho_R = f_R/(2kT) \tag{A4b}$$

and

$$\rho_a = \rho_R f_b/f_R \tag{A5a}$$

$$\rho_b = \rho_R(2/f_R)[1/f_a + 1/f_b]^{-1} \tag{A5b}$$

Note that disorientation of the long axis (ρ_a) involves rotations about the short axes only, where disorientation of the short axis (ρ_b) involves contributions from rotations about the long axis and the other short axis as well.

In general, the observed rotational relaxation time, ρ_h, is an average value, weighted by the angle β between the emission dipole and the axis of revolution of the ellipsoid (Weber, 1953).

$$1/\rho_h = [(\cos^2 \beta)/\rho_a + (1 - \cos^2 \beta)/\rho_b] \tag{A6}$$

For a random distribution of fluorophores, the average $\cos^2 \beta = {}^1/_3$ and the following equation results:

$$1/\rho_h = {}^1/_3(1/\rho_a + 2/\rho_b) \tag{A7}$$

In the limit of a long prolate ellipsoid, p approaches 0 and eq A2a reduces to

$$\text{limit } p \to 0: \quad f_a = {}^2/_3 f_R \tag{A8}$$

whereas f_b increases without limit, i.e., $f_b \to \infty$. Thus $\rho_a \to \infty$ as well, from eq A5a. Examination of eq A5b and A7 indicates that in the limit of an infinitely long ellipsoid

$$\text{limit } p \to 0: \quad \rho_b = {}^4/_3 \rho_R \tag{A9}$$

$$\text{limit } p \to 0: \quad \rho_h = 2\rho_R \tag{A10}$$

That is, a very long prolate ellipsoid is characterized by a single rotational relaxation time equal to twice the value for a spherical molecule of equivalent volume.

The consequences of nonrandom orientation of the fluorophore can be ascertained from eq A6. In one case, if the fluorophore is attached parallel to the long (a) axis of the ellipsoid, $\cos^2 \beta = 1$ and eq A6 reduces to

$$\text{fluorophore parallel to the } a \text{ axis:} \quad \rho_h = \rho_a \tag{A11}$$

Note that as $p \rightarrow 0$, ρ_h increases without bound.

In the other extreme, of the fluorophore attached parallel to one of the two equivalent short axes (b), $\cos^2 \beta = 0$ and eq A6 becomes

$$\text{fluorophore parallel to either } b \text{ axis:} \quad \rho_h = \rho_b \tag{A12}$$

Note that in this case, eq A9 indicates that in the limit of a very long ellipsoid, with the probe attached to either b axis

$$\text{limit } p \rightarrow 0: \quad \rho_h = {}^4/_3\rho_R \tag{A13}$$

References

Cantor, C. R., & Schimmel, P. R. (1980) in *Biophysical Chemistry*, Part II, pp 562–563, W. H. Freeman, San Francisco, CA.

Carr, M. E., & Hermans, J. (1978) *Macromolecules 11*, 46–50.

Chen, R., & Doolittle, R. F. (1971) *Biochemistry 10*, 4486–4491.

Chen, R. F., Edelhoch, H., & Steiner, R. F. (1969) in *Physical Principles and Techniques of Protein Chemistry* (Leach, S. J., Ed.) Part A, pp 171–244, Academic Press, New York.

Cottrell, B. A., Strong, D. D., Watt, K. W. K., & Doolittle, R. F. (1979) *Biochemistry 18*, 5405–5410.

Donovan, J. W., & Mihalyi, E. (1974) *Proc. Natl. Acad. Sci. U.S.A. 71*, 4125–4128.

Doolittle, R. F. (1973) *Adv. Protein Chem. 27*, 1–109.

Doolittle, R. F. (1977) *Horiz. Biochem. Biophys. 3*, 164–191.

Doolittle, R. F. (1980) in *Clinical Laboratory Science* (Schmidt, R. M., Ed.) Vol. III, Sect. I (Hematology) pp 3–14, CRC Press, Boca Raton, FL.

Doolittle, R. F., Goldbaum, D. M., & Doolittle, C. R. (1978) *J. Mol. Biol. 120*, 311–325.

Doolittle, R. F., Watt, K. W. K., Cottrell, B. A., Strong, D. D., & Riley, M. (1979) *Nature (London) 280*, 464–468.

Fair, D. S., Edgington, T. G., & Plow, E. F. (1981) *J. Biol. Chem. 256*, 8018–8023.

Fowler, W. E., & Erickson, H. P. (1979) *J. Mol. Biol. 134*, 241–249.

Fowler, W. E., Fretto, L. J., Erickson, H. P., & McKee, P. A. (1980) *J. Clin. Invest. 66*, 50–56.

Fowler, W. E., Erickson, H. P., Hantgan, R. R., McDonagh, J., & Hermans, J. (1981a) *Science (Washington, D.C.) 211*, 287–289.

Fowler, W. E., Hantgan, R. R., Hermans, J., & Erickson, H. P. (1981b) *Proc. Natl. Acad. Sci. U.S.A. 78*, 4872–4876.

Hall, C., & Slayter, H. (1959) *J. Biochem. Biophys. Cytol. 5*, 11–15.

Hantgan, R. R. (1981) *Thromb. Haemostasis 46*, 160.

Hantgan, R. R., & Hermans, J. (1979) *J. Biol. Chem. 254*, 11272–11281.

Henschen, A., & Lottspeich, F. (1980) *Hematologia 65*, 535–541.

Hudry-Clergeon, G., Marguerie, G., Pouit, L., & Suscillon, M. (1975) *Thromb. Res. 6*, 533–541.

Johnson, P., & Mihalyi, E. (1965) *Biochim. Biophys. Acta 102*, 476–486.

Kanaide, H., & Shainoff, J. R. (1975) *J. Lab. Clin. Med. 85*, 574–597.

Kettner, C., & Shaw, E. (1977) in *Chemistry and Biology of Thrombin* (Lundblad, R. L., Fenton, J. W., & Mann, K. G., Eds.) pp 129–142, Ann Arbor Science, Ann Arbor, MI.

Laki, K., & Lorand, L. (1948) *Science (Washington, D.C.) 108*, 220.

Lakowicz, J. R., Prendergast, F. G., & Hogen, D. (1979) *Biochemistry 18*, 508–519.

Lentz, B. R., Freire, E., & Biltonen, R. L. (1978) *Biochemistry 17*, 4475–4480.

Lorand, L., Ong, H. H., Lipinski, B., Rule, N. G., Downey, J., & Jacobsen, A. (1966) *Biochem. Biophys. Res. Commun. 25*, 629–637.

Lorand, L., Downey, J., Gotoh, T., Jacobsen, A., & Tokura, S. (1968a) *Biochem. Biophys. Res. Commun. 31*, 222–230.

Lorand, L., Rule, N. G., Ong, H. H., Furlanetto, R., Jacobsen, A., Downey, J., Oner, N., & Bruner-Lorand, J. (1968b) *Biochemistry 7*, 1214–1223.

Lorand, L., Urayama, T., deKiewitt, J. W. C., & Nossel, H. L. (1969) *J. Clin. Invest. 48*, 1054–1064.

Lorand, L., Lockridge, O. M., Campbell, L. K., Myrhman, R., & Bruner-Lorand, J. (1971) *Anal. Biochem. 44*, 221–231.

Lorand, L., Chenoweth, D., & Gray, A. (1972) *Ann. N.Y. Acad. Sci. 202*, 155–171.

Marder, V. J., Shulman, N. R., & Carroll, W. R. (1969) *J. Biol. Chem. 244*, 2111–2119.

Marguerie, G. (1979) *Thromb. Haemostasis 41*, 635–641.

McClure, W. O., & Edelman, G. M. (1966) *Biochemistry 5*, 1908–1919.

McDonagh, J., & McDonagh, R. P. (1980) in *Clinical Laboratory Science* (Schmidt, R. M., Ed.) Vol. III, Sect I (Hematology) pp 125–140, CRC Press, Boca Raton, FL.

Mihalyi, E. (1981) *Thromb. Haemostasis 46*, 356.

Mihalyi, E., & Albert, A. (1971a) *Biochemistry 10*, 237–242.

Mihalyi, E., & Albert, A. (1971b) *Biochemistry 10*, 243–249.

Perrin, F. (1934) *J. Phys. 5*, 497–511.

Pisano, J. J., Finlayson, J. S., & Peyton, M. P. (1969) Biochemistry *8*, 871–876.

Pulleybank, D. E., Shure, M., & Vinograd, J. (1977) *Nucleic Acids Res. 4*, 1409–1419.

Serrallach, E. N., Hofmann, V. E., Zulauf, M., Binkert, T., Hofmann, R., Kanzig, W., Straub, P. W., & Schwyzer, R. (1979) *Thromb. Haemostasis 41*, 648–654.

Steiner, R. F., & McAlister, A. J. (1957) *J. Polym. Sci. 24*, 105–123.

Stryer, L. (1965) *J. Mol. Biol. 13*, 482–495.

Takagi, T., & Doolittle, R. F. (1975) *Biochemistry 14*, 5149–5156.

Tao, T. (1969) *Biopolymers 8*, 609–632.

Wahl, P., & Weber, G. (1967) *J. Mol. Biol. 30*, 371–382.

Weber, G. (1953) *Adv. Protein Chem. 8*, 415–459.

Weisel, J. W., Phillips, G. N., & Cohen, C. (1981) *Nature (London) 289*, 263–267.

Williams, R. C. (1981) *J. Mol. Biol. 150*, 399–408.

Yguerabide, J., Epstein, H. F., & Stryer, L. (1971) *J. Mol. Biol. 51*, 573–590.